Food Bioscience 61 (2024) 104887

Contents lists available at ScienceDirect

Food Bioscience

journal homepage: www.elsevier.com/locate/fbio

Dietary chromium chemical species mitigate inflammation and cholestasis in primary sclerosing cholangitis via regulating bile acid metabolism

Yu Shen [a], Baorong Jiang [a], Zejia Hao [a], Chenchen Zhang [a], Zhan Zhang [a,b], Qian Wu [a,b], Lei Li [a,b,**], Ping Jiang [a,b,*]

[a] Center for Global Health, School of Public Health, Nanjing Medical University, 101 Longmian Avenue, Nanjing, Jiangsu, 211166, PR China
[b] The Key Lab of Modern Toxicology of Ministry of Education, School of Public Health, Nanjing Medical University, 101 Longmian Avenue, Nanjing, Jiangsu, 211166, PR China

ARTICLE INFO

Keywords:
Cr-pic
$CrCl_3$
PSC
Inflammation
Bile acid metabolism
Gut microbiota

ABSTRACT

Both chromium picolinate (Cr-pic) and chromium trichloride ($CrCl_3$) were used as dietary supplements in agricultural products and foodstuffs. We found either these two forms of Cr(III) could ameliorate inflammation and cholestasis in DDC-induced primary sclerosing cholangitis (PSC) mice via regulating bile acid metabolism. Although two Cr(III) are able to alleviate hepatic inflammation by reducing the aggregation of macrophage, Cr-pic exhibiting superior efficacy in decreasing M1 macrophages. Two Cr(III) show inconsistent in regulating intestinal *Fxr*, but Cr-pic could active intestinal *Fxr*, promoting intestinal barrier repair. Additionally, both Cr-pic and $CrCl_3$ enhanced functional abundance of BSH enzymes involved in bile acid transformation, with Cr-pic seems to perturb the abundance of genus more than $CrCl_3$. In conclusion, this study highlights the efficacy of Cr-pic and $CrCl_3$ in mitigating inflammation and cholestasis in PSC, Cr-pic is expected superior than $CrCl_3$ to be supplement ingredient used in PSC treatment via regulating bile acid metabolism.

1. Introduction

Trivalent chromium (Cr(III)) is extensively utilized as dietary supplements for both human and animal feed, and can be classified into organic and inorganic species. There are many organic varieties of Cr (III) widely used in foodstuff as nutritional supplements and flavoring agent, including chromium picolinate (Cr-pic), chromium malate (Cr-mal), chromium yeast and chromium nicotinate (Cr-nic), etc. Cr-pic is mainly applied as a nutritional supplement, playing a crucial role in weight management and the treatment of diabetes, act as a regulatory factor influencing insulin tolerance and actively participating in glucose and lipid metabolism(Willoughby, Hewlings, & Kalman, 2018; Zheng, Hu, Shao, Chen, & Qi, 2023). Cr-pic (up to 200 μg/L Cr) is allowed as swine feed additive to improve carcass leanness and reproductive efficiency in United States(Mooney & Cromwell, 1997; White & Vincent, 2019). In addition, previous study has certificated 200, 400, 800 μg Cr-pic/kg diet could reduce total cholesterol (TC) and increased low density lipoprotein (LDL) in laying hens(White et al., 2019). Cr-mal diet (15.0 and 20.0 μg Cr/kg bw/day) could significantly reduce the levels of TC and triglyceride (TG) of male type 2 diabetic rats(Feng et al., 2019). Cr yeast (200 μg Cr in morning, 100 μg in evening) could significantly reduce resting heart rate in patients with metabolic syndrome and impaired glucose tolerance (IGT), which could represent a cardiovascular risk reduction in patients with high cardiometabolic risk(Nussbaumerova et al., 2018). Moreover, Cr chloride ($CrCl_3$), an inorganic oxidative form of Cr(III) also could inhibit insulin resistance in palmitic acid-treated HepG2 cells by increased *PPARγ* (100 μM Cr), which suggests that $CrCl_3$, similar to organic trivalent chromium, can also play a role in body metabolism(Nishimura, Iitaka, & Nakagawa, 2021). However, studies have demonstrate that the dietary organic Cr(III) (Cr-pic) had significantly higher bioaccumulation than inorganic Cr(III) ($CrCl_3$), further prompt Cr-pic and $CrCl_3$ seem have distinct fucntions to in terms of regulation of metabolism(Li et al., 2022). Recent years have witnessed an increased focus on the role of bile acids as signaling molecules in

* Corresponding author. Center for Global Health, School of Public Health, Nanjing Medical University, 101 Longmian Avenue, Nanjing, Jiangsu, 211166, PR China.
** Corresponding author. Center for Global Health, School of Public Health, Nanjing Medical University, 101 Longmian Avenue, Nanjing, Jiangsu, 211166, PR China.
E-mail addresses: lilei@njmu.edu.cn (L. Li), jiangping@njmu.edu.cn (P. Jiang).

https://doi.org/10.1016/j.fbio.2024.104887
Received 7 June 2024; Received in revised form 31 July 2024; Accepted 4 August 2024
Available online 6 August 2024

regulating host glucose and lipid metabolism, including in emulsifying and absorbing dietary fats and other lipophilic compounds(Cai, Rimal, Jiang, Chiang, & Patterson, 2022; Lin et al., 2023; Sun, Fan, Li, Yan, & Jiang, 2022; Tveter, Mezhibovsky, Wu, & Roopchand, 2023). Therefore, we speculated that Cr-pic and $CrCl_3$ intervention may influence bile acid metabolism participate in regulating body metabolism.

To investigate how organic and inorganic Cr(III) regulates bile acid metabolism, we selected primary sclerosing cholangitis (PSC) as an experimental model. PSC is a cholestatic disease arising from disruptions in bile acid metabolism and is characterized by multifocal bile duct strictures, inflammation and fibrosis around the bile ducts(Y. S. Kim, Hurley, Park, & Ko, 2023; Lin et al., 2023; Little, Wine, Kamath, Griffiths, & Ricciuto, 2020). Epidemiology shows that the incidence of PSC is 1–1.5 per 100,000 person-years and the prevalence is 6–16 per 100,000 person-years, both may increase over time(Assis & Bowlus, 2023). Currently, research on the interaction between trivalent chromium and cholestasis is virtually nonexistent. Our previous study has found that 1 mg/L Cr(III) exposure for 120 h could disturb metabolism pathway of primary bile acid biosynthesis in zebrafish, thus we speculate Cr-pic and $CrCl_3$ may have function in regulation of bile acid metabolism. Furthermore, since PSC patients often have inflammatory bowel disease, especially ulcerative colitis, the occurrence of PSC due to intestinal inflammation was considered(Ali, Carey, & Lindor, 2016). Intestinal inflammation increases intestinal permeability, which induce bacteria and their products may travel with the blood into the portal system to the liver, and cause inflammation in the portal region(Di Vincenzo, Del Gaudio, Petito, Lopetuso, & Scaldaferri, 2023). Researchers have noted that the gut microbiota composition in individuals with PSC differs from that of healthy individuals, with reduced gut bacterial alpha diversity in PSC compared to healthy controls(Hov & Karlsen, 2023; Little et al., 2020). In this study, we used 3,5-diethoxycarbonyl-1,4-dihydrocollidine (DDC) supplemented diet induce PSC mouse model which could induce intrahepatic porphyrin obstruction resulting in emergence of spontaneous cholestatic symptoms accompany with inflammation and fibrosis in liver(Deng et al., 2018; Fickert et al., 2007; S. Zheng, Cao, et al., 2021). Both organic and inorganic Cr(III) intervention demonstrates remarkable benefits in mitigating liver injury, reducing inflammation, and restoring cholestasis in PSC mice via regulating bile acid metabolism. With the effect on specific bile acid level and gut microbiota, Cr-pic and $CrCl_3$ showed inconsistent results, Cr-pic demonstrates superior efficacy than $CrCl_3$ in influencing bile acid homostasis, modulating gut microbiota composition and improving intestinal damage. These findings will be available to explore the application value of Cr-pic is superior to $CrCl_3$ in alleviate PSC symptom.

2. Materials and methods

2.1. Animal experiments

7-Week-old male C57BL/J specific pathogen free (SPF) mice were purchased from GemPharmatech Co., LTD., housed with a 12-h light/dark cycle, with no restrictions on their food or water under conditions of controlled humidity (50% ± 5%) and temperature (22 ± 2 °C). All the experimental programs for mice have been approved by the Nanjing Medical University Institutional Animal Care and Use Committee (Approval No. IACUC-2311028). A total of 60 mice were randomly divided into 6 groups with 10 mice in each group for experimental treatment. Specific grouping and treatment are as follows: six groups, control, Cr-pic, $CrCl_3$, DDC, DDC-Cr-pic and DDC-$CrCl_3$ with 10 mice in each group. Mice in control, Cr-pic and $CrCl_3$ group were fed normal diet all the time, then control mice were given ddH_2O. After 5 days, Cr-pic and $CrCl_3$ group mice daily gavage 75 μg chromium/kg B.W., referencing the recommended daily intake for humans as outlined in the literature and the intake levels used in rodent studies(Vincent & Lukaski, 2018). Mice in DDC, DDC, DDC-Cr-pic and DDC-$CrCl_3$ group were fed a customized diet (synthesized by Xietong Pharmaceutical Bio-engineering, Jiangsu, China) for 12 days by feeding 0.1% (w/w) DDC (CAS: 632-93-9; Sigma-Aldrich Co., LTD.) to construct PSC mouse model. Then, three groups were given ddH_2O/chromium (chromium picolinate (Cr-pic, AR, CAS: 14639-45-9) and chromium chloride hexahydrate ($CrCl_3{\cdot}6H_2O$, AR, CAS:10060-12-5) purchased from Shanghai Aladdin Biochemical Technology Co., Ltd) gavage for one week. Weight was recorded daily from the first day of the experiment. Fresh feces were collected, and all the mice were sacrificed after 12 h of starvation at the last day. The collected blood was placed at 4 °C for 12 h and centrifuged to collect serum. The liver was excised immediately and then divided, sections were fixed and sliced for further histological analysis, the rest was stored at −80 °C until use.

2.2. Biochemical parameters analysis of serum

Serum biochemical parameters, aspartate aminotransferase (AST), alanine aminotransferase (ALT), alkaline phosphatase (ALP), total bilirubin (TBIL), and total bile acid (TBA), were analyzed using an automated biochemical analyzer (Hitachi 7100, Tokyo, Japan).

2.3. Histopathology

The liver and intestinal tissues were fixed with 4% paraformaldehyde (Servicebio, Wuhan, China) for more than 24 h. Tissues from each mouse were then paraffin embedded, cut into 4 μm thick and stained with haematoxylin and eosin (H&E), sirius red (SR) and immunohistochemical (IHC) staining. The Histology of the ileum based on H&E staining were scored according to the procedures of published literature (Ma et al., 2023). The IHC staining was used to analyze CD11b (rabbit anti-CD11b, GB11058-100, Servicebio, Wuhan, China). Standard procedures of IHC staining were used as described in a previous study(Shen et al., 2023). According to standard procedures, the main experimental steps included fixing, paraffinizing, deparaffinizing, dehydrating, antigen retrieval, blocking endogenous peroxidase activity, sealing, primary antibody incubation, washing, sealing, secondary antibody incubation, washing, chromogenic, nucleus counterstaining, dehydration and mounting, and observation. Pannoramic scanning (3DHISTECH, Budapest, Hungary) was used to obtain representative images by blind scanning the stained slides. The images were then analyzed and quantified using ImageJ (2.9.0, Bethesda, USA).

2.4. Tissue RNA extraction and qPCR for gene expression

Total RNA was extracted from liver and ileum using Trizol (Tiangen, Beijing, China) and reverse transcribed into cDNA using HiScript II Q RT SuperMix (Vazyme Biotech, Nanjing, China). The concentration and purity of total RNA were measured by NanoDrop 2000 spectrophotometer. The primers were synthesized by genscript (Nanjing, China). The mixture was subject to qPCR on Roche Lightcycler 480 (Basel, Switzerland). RT-qPCR analysis was performed in triplicate. Gapdh was used as the internal control for the expression level of target genes, and the relative expression level was evaluated using $2^{-\Delta\Delta Ct}$ method.

2.5. Flow cytometry

Antibodies are indicated as follows: anti-mouse CD45 eFluor450 (48-0451-82, eBioscience, San Diego, CA, USA), anti-mouse F4/80 PE (12-4801-82, eBioscience), anti-mouse CD11b FITC (11-0112-82, eBioscience), and anti-mouse CD16/CD32 PerCP-Cyanine5.5 (45-0161-80, eBioscience). To determine the specificity of the FCM results, fluorescence-minus-one controls were performed according to the approaches as described. Cells were blocked for 15 min at 4 °C before adding the other antibodies.The tests were detected by FACSymphony A5 SORP, and the data were analyzed using FlowJo 10.8.1 software.

2.6. Measurement of TBAs in serum, liver and intestine

The levels of total bile acids (TBAs) in liver and intestine were detected using TBAs kits (No. E003–2-1; Jiancheng Bioengineering Institute, Nanjing, China) according to the manufacturer's protocol.

2.7. Western blot

Liver samples underwent protein extraction dedicated kit from KeyGEN Biotech (KGB5303-100), with protein concentrations precisely quantified using BCA assay reagents from KeyGEN Biotech (KGB2101-250). Following extraction, protein samples were subjected to denaturation at 95 °C for 5 min in an upwelling buffer. Samples were then resolved via 10% SDS-PAGE electrophoresis and transferred onto polyvinylidene difluoride (PVDF) membranes sourced from Millipore (Billerica, MA, USA). The PVDF membranes were incubated overnight at 4 °C with rabbit anti-FXR (1:1000, Proteintech, 25055-1-AP) or rabbit anti-GAPDH (1:1000, Proteintech, 10494-1-AP). Subsequently, the membranes were treated with secondary antibodies, enabling the visualization of immune complexes through an enhanced chemiluminescence immunoblotting assay (Vazyme, E411-04).

2.8. Targeted determination of BAs using LC/MS

The analysis of bile acids (BAs) types and contents in stool, liver and serum samples involved liquid chromatography-mass spectrometry (LC-MS). Initially, a mixed standard liquid was prepared by weighing standard substances, adding methanol to a constant volume, and obtaining the reserve liquid through thorough mixing. A working solution was then prepared by diluting the mixed standard liquid with 50% methanol. Subsequently, 20 mg of the stool and liver sample were accurately weighed, and 400 μL of the extract (methanol:water = 4:1) was added. The sample was ground for 6 min at −20 °C and 60 Hz using a frozen tissue grinding machine, followed by a 30-min ultrasonic treatment at 4 °C. After standing for 30 min at −20 °C, the mixture was centrifuged for 15 min at 4 °C and 12000 rpm. Finally, 200 μL of the supernatant was collected and analyzed. For serum samples, 50 μL was taken and mixed with 150 μL of methanol. Subsequently, ultrasonication was performed at 4 °C for 30 min. After standing for an additional 30 min at −20 °C, the mixture underwent centrifugation at 4 °C and 12000 rpm for 15 min. Finally, 150 μL of the supernatant was collected and subjected to analysis.

2.9. 16S rRNA sequence

Microbial community genomic DNA was extracted from stool samples and assessed for quality through electrophoresis on a 1% agarose gel. The concentration and purity of DNA were determined using a NanoDrop 2000 UV–vis spectrophotometer (Thermo Scientific, Wilmington, USA). The V3–V4 hypervariable region of the bacterial 16S rRNA gene was amplified with an ABI GeneAmp® 9700 PCR thermocycler (ABI, CA, USA). Sequencing was performed on an Illumina MiSeq platform (PE300), and data analysis was conducted on the Majorbio Cloud Platform (www.majorbio.com). Principal coordinate analysis (PCoA) was carried out based on operational taxonomic units (OTU) levels utilizing Bray-Curtis dissimilarity.

2.10. Statistical analysis

The data in this study were expressed as mean ± standard deviation (SD). Statistical comparisons were analyzed using GraphPad Prism 9 (La Jolla, USA). Homogeneity of variance was tested using Levene's test, then *t*-test was carried out to calculate significant differences between groups. Kruskal–Wallis test was used when data did not follow a normal distribution.The data were plotted using GraphPad Prism 9. $p < 0.05$ was considered statistically significant.

3. Result

3.1. Cr-pic and $CrCl_3$ supplementation attenuated liver damage and fibrosis in PSC mice

In the scenario depicted in Fig. 1A, mice were subjected to 0.1% (w/w) DDC-diet for 5 days with subsequent interferes with Cr-pic and $CrCl_3$ respectively for one week and continue the DDC dietary intervention during this week. In comparison to the control group, the DDC group mice exhibited a significant decline in body weight starting from the second day (Fig. 1B), whereas the intervention of organic and inorganic Cr(III) did not yield any discernible effects. The DDC-induced condition led to heightened levels of ALT and AST (Fig. 1C), which signal liver injury in PSC mice. These markers exhibited diminished levels in the DDC-Cr-pic and DDC-$CrCl_3$ groups as opposed to the DDC group (Fig. 1C), which suggest that liver injury in PSC mice was ameliorated by the involvement of Cr(III). Through SR staining, DDC exposure also triggered onion-skin fibrosis in liver, a distinct trait of PSC (Fig. 1D). Notably, both organic and inorganic Cr(III) interventions mitigated fibrosis of PSC mice. Subsequent qPCR analyses unveiled the elevation of collagen type I alpha 1 (*Collagen 1a1*) and matrix metalloproteinase-9 (*Mmp9*) induced by DDC were curtailed by Cr-pic and $CrCl_3$ interventions in liver (Fig. 1E). Additionally, the intervention of Cr-pic and $CrCl_3$ also reduced the high levels of α-smooth muscle actin (*αSMA*), transforming growth factor beta 1(*Tgfβ1*, a key cytokine inducing fibrosis), and transforming growth factor beta receptor 1(*Tgfβr1*) expression in the liver of PSC mice, indicating that Cr-pic and $CrCl_3$ can alleviate liver fibrosis in PSC mice by decreasing the expression of *Tgfβ1* and its receptor *Tgfβr1*, thereby inhibiting the expression of *αSMA* (Katanasaka et al., 2024). These data collectively demonstrated Cr-pic and $CrCl_3$ notably improved both DDC-induced liver injury and fibrosis.

3.2. Organic and inorganic Cr(III) alleviated liver inflammation in PSC mice through macrophages and the M1 polarized-macrophages significantly decreased in DDC-Cr-pic group

No matter organic nor inorganic Cr(III) intervention did not induce inflammation in the liver of control mice (Fig. 2A). In PSC mice, there was a significant accumulation of inflammatory cells around the bile ducts, following Cr-pic and $CrCl_3$ intervention, there was a reduction in inflammatory cells (Fig. 2A). In addition to the histological observations, we assessed the improvement in inflammation by measuring the expression levels of inflammatory cells biomarkers in liver tissues using qPCR. Compared to the DDC group, the monocyte chemoattractant factor (*Mcp-1*) significantly decreased in mice subjected to organic and inorganic Cr(III) intervention (Fig. 2C). This suggests that both Cr-pic and $CrCl_3$ intervention reduces the chemotaxis and aggregation of monocytes induced by DDC, thereby alleviating inflammation driven by monocytes. Similar changes were also observed in the expression levels of vascular cell adhesion molecule (*Vacm-1*), which were significantly reduced in both DDC-Cr-pic and DDC-$CrCl_3$ groups compared to the DDC group (Fig. 2C). These results collectively indicate that both Cr-pic and $CrCl_3$ intervention significantly reduces the release of inflammatory cell-related factors, sequentially improving liver inflammation in PSC mice. Immunohistochemical results for CD11b in mice liver tissues (Fig. 2B) showed a marked increase in CD11b-positive areas in the livers of PSC mice, which decreased after organic and inorganic Cr(III) intervention (Fig. 2B–D). Flow cytometry (FCM) analysis of $F4/80^+CD11b^+$ macrophages in mice liver tissues revealed that, compared with DDC group, both Cr-pic and $CrCl_3$ could reduce the number of $F4/80^+CD11b^+$ macrophages in PSC mice livers (Fig. 2E–G). These results indicate that both Cr-pic and $CrCl_3$ can reduce the number of macrophages in the liver. Analysis of $CD16/32^+F4/80^+CD11b^+$ M1-polarized macrophages in liver and the measurement of M1-polarized macrophage factors showed that in PSC mice, there was a significant increase in M1-polarized macrophages compared to the control group (Fig. 2F–H).

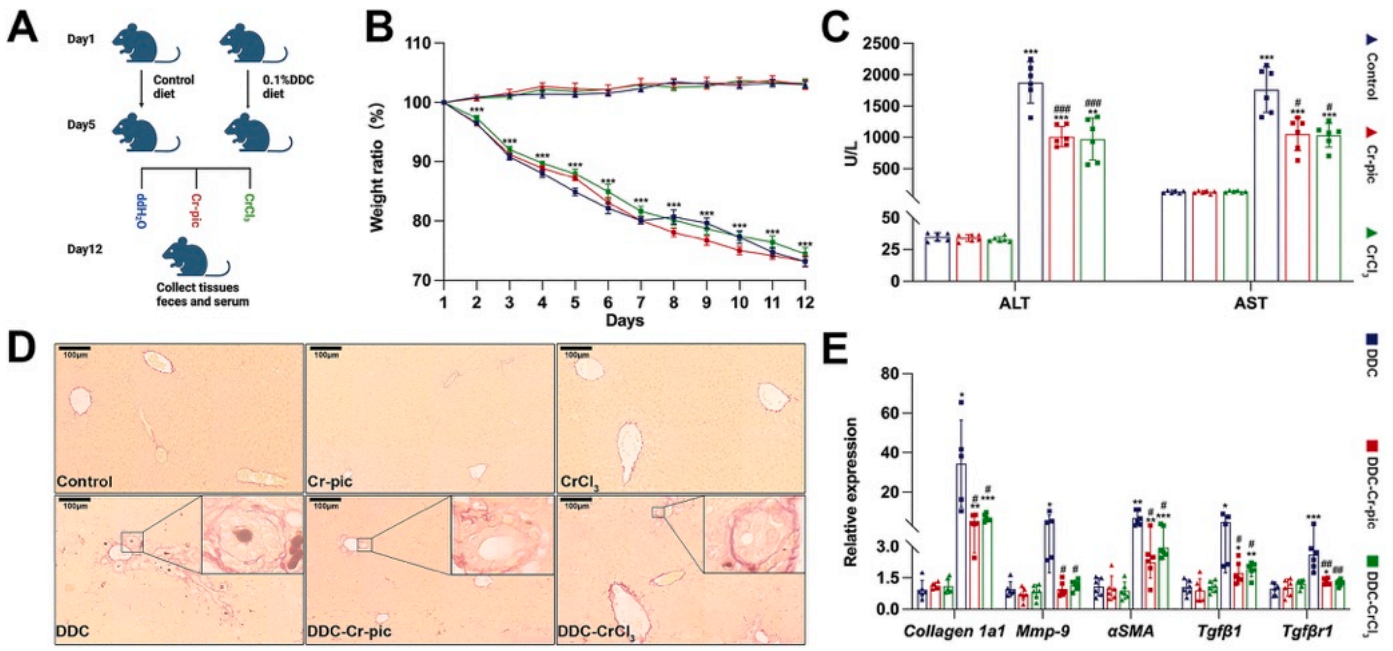

Fig. 1. The effect of Cr-pic and $CrCl_3$ intervention on the disease phenotype of PSC mice. (A) Schematic diagram of PSC mouse construction and intervention method in this experiment. (B) Changes in body weight ratio of each group of mice over 12 days. (C) The serum levels of ALT and AST of mice in each group. (D) SR-stained pathological sections of the liver of each group. All scales are 100 μm. (E) Expression of fibrosis-related factors (*Collagen-1a1*, *Mmp-9*, *αSMA*, *Tgfβ1* and *Tgfβr1*) in liver of each group. (* is the statistical difference compared with the control group, and # is the statistical difference compared with the DDC group; $^{*}p < 0.05$, $^{**}p < 0.01$, $^{***}p < 0.001$; $\#p < 0.05$, $\#\#p < 0.01$).

However, Cr-pic intervention could reduce the number of M1-polarized macrophages and suppress the expression of their factors tumor necrosis factor α (*Tnfα*), inducible nitric oxide synthase (*iNOS*) and chemokine C-X-C ligand 10 (*Cxcl10*) in PSC mice(Fig. 2I). $CrCl_3$ exhibited a trend towards downregulating Tnfα and iNOS, but no significant differences were observed. The aforementioned findings collectively illustrate that $CrCl_3$ and Cr-pic effectively mitigates macrophage accumulation in the livers of PSC mice to alleviate inflammation. Additionally, organic Cr (III) Cr-pic displays a notable capacity to mitigate liver inflammation to a greater extent by reducing the population of M1-polarized macrophages and suppressing factor expression.

3.3. Cr-pic and $CrCl_3$ improved DDC-induced liver cholestasis disturbed via regulating bile acid metabolism disfunction in PSC mice, Cr-pic exerted additional regulation in intestine

To investigate the effect of organic and inorganic Cr(III) intervention on bile acid metabolism, blood biochemistry test showed that the serum ALP index increased significantly in the DDC group compared with the control group and decreased significantly under the intervention of Cr-pic and $CrCl_3$ Cr(III) compared to DDC, which demonstrated that both Cr-pic and $CrCl_3$ was able to attenuate the cholestasis in PSC mice (Fig. 3A). Studies showed that the elevation of alkaline phosphatase isoenzyme (ALP) that distributed in the capillary bile duct of liver cells helps to identify cholestasis related diseases(Zhao et al., 2017). We further assessed total bilirubin (TBIL) and total bile acid (TBA) levels in blood, as well as TBA concentrations in the liver and small intestine. Serum TBIL and TBA levels were notably elevated in DDC-induced PSC mice compared to the control group, yet both organic and inorganic Cr (III) interventions led to significant reductions in PSC mice (Fig. 3B). While liver TBA levels surged in PSC mice, small intestine bile acid content showed a distinct decline. After organic and inorganic Cr(III) intervention, liver TBA levels notably decreased, and the DDC-Cr-pic mice exhibited a remarkable rebound in small intestine TBA levels compared to DDC group (Fig. 3C). $CrCl_3$ intervention didn't restore deficient bile acids in small intestine caused by intrahepatic cholestasis. These findings underscore both organic and inorganic Cr(III) could regain serum and liver bile acid equilibrium, but Cr-pic intervention effectively replenished missing bile acids in the small intestine. Therefore, we speculate Cr-pic could recover cholestasis in both intrahepatic and intra-intestinal which expected to be used as an adjunct to relieve cholestasis. To elucidate the mechanism of Cr-pic and $CrCl_3$ intervening in improving PSC mice bile acid metabolism, we detected genes expression of bile acid synthesis and transport pathways in the liver and small intestine. Results revealed that Cr-pic and $CrCl_3$ interventions prominently elevated liver farnesoid x receptor (*Fxr*) expression in PSC mice, and then suppressing recombinant Cytochrome P450 7A1 (*Cyp7a1*) to reducing liver bile acid synthesis (Fig. 3D–F). Furthermore, both Cr-pic and $CrCl_3$ intervention curbed sodium taurocholate cotransporting polypeptide (*Ntcp*) and organic anion transporting polypeptide 4 (*Oatp4*) in PSC mice to activate bile acid transporters (e.g., peroxisome proliferative activated receptor alpha (*PPARα*), multidrug resistance associated protein 2 (*Mrp2*) and *Mrp3* expedited bile movement (Fig. 3G and H) and alleviating intrahepatic cholestasis. Remarkably, organic Cr(III) Cr-pic could activate apical sodium-dependent bile acid transporter (*Asbt*) in the small intestine of PSC mice (Fig. 3I). This activated *Fxr* in small intestine, stimulating liver fibroblast growth factor receptor4 (*Fgfr4*) (Fig. 3D–J), ultimately repressing *Cyp7a1* through *Fxr* activation and reducing hepatic bile acid synthesis. In summary, both Cr-pic and $CrCl_3$ effectively mitigates bile acid metabolism disorders in PSC mice, with organic Cr(III) Cr-pic demonstrating superior efficacy in the intestine compared to inorganic Cr(III) $CrCl_3$.

3.4. Cr-pic and $CrCl_3$ restored the decline in HCA level caused by DDC, Cr-pic extraly modulated CDCA and T-βMCA

To explore detailed bile acid alteration associated with organic and inorganic Cr(III) interventions, we conducted a comprehensive analysis of 47 bile acid species in mouse feces to monitor variations. A visual representation in the form of a pie chart depicted their distribution, which categorized these bile acids into two groups: conjugated (bound to taurine or glycine) and unconjugated bile acids (Fig. 4A). In

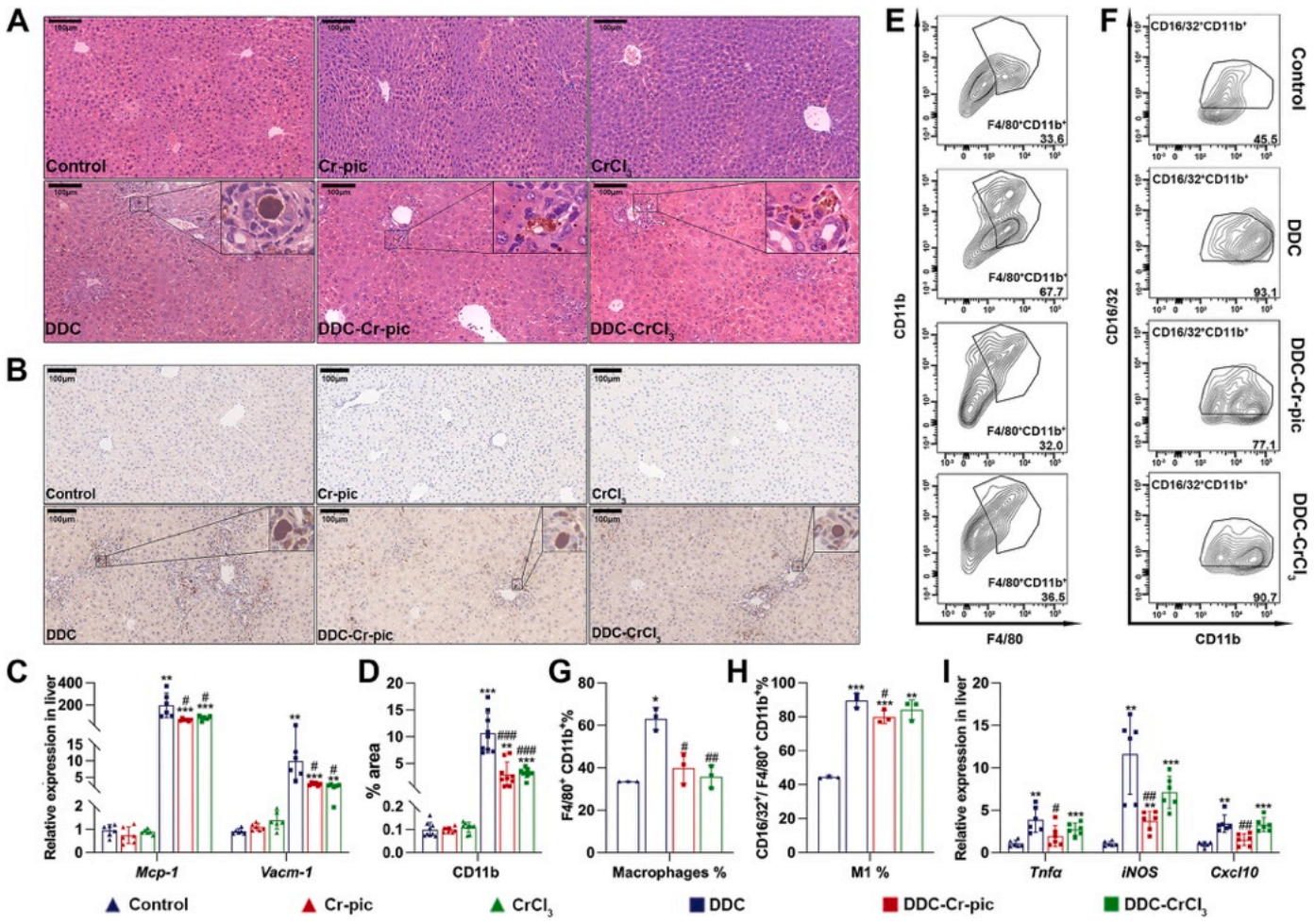

Fig. 2. The effect of Cr-pic and $CrCl_3$ on improving liver inflammation in PSC mice. (A) H&E staining of the livers. (B) Immunohistochemical staining of CD11b in liver. (C) Expression of inflammatory cell factors *Mcp-1* and *Vacm-1* in liver. (D) Proportion of CD11b-positive areas in immunohistochemical staining. (E) Representative FCM results of $F4/80^+CD11b^+$ cells in liver. (F) Representative FCM results of $CD16/32^+F4/80^+CD11b^+$ cells in liver. (G) Quantification of $F4/80^+CD11b^+$ cells in liver. (H) Quantification of $CD16/32^+F4/80^+CD11b^+$ cells in liver. (I) Expression levels of M1 polarization-related cytokines *Tnfα, iNOS* and *Cxcl10* in liver. (* is the statistical difference compared with the control group, and # is the statistical difference compared with the DDC group; $*p < 0.05$, $**p < 0.01$, $***p < 0.001$; $\#p < 0.05$, $\#\#p < 0.01$, $\#\#\#p < 0.001$).

comparison to the control group, DDC mice exhibited diminished levels of conjugated bile acids, and the intervention of Cr-pic and $CrCl_3$ could not entirely restore this change. Intriguingly, deconjugated bile acids were notably higher in DDC-Cr-pic mice compared to DDC group (Fig. 4B), implying that organic Cr(III) Cr-pic could effectively regulate the level of unconjugated bile acids to relieve cholestasis in the intestine. Among these bile acids, two unconjugated bile acids, chenodeoxycholic acid (CDCA) and hyodeoxycholic acid (HCA), declined obviously induced by DDC compared with control (Fig. 4C). On the contrary, Cr-pic intervention could partly recover the level of CDCA and HCA and only a small amount of HCA level can be restored by $CrCl_3$. Furthermore, PSC mouse liver and serum displayed notably elevated HCA levels (Fig. 4D and E), which were mitigated by both organic and inorganic Cr (III) interventions. Therefore, we think Cr(III) participates in regulation of bile acid content and composition by modulating changes in HCA content. In addition, DDC diet decreased two conjugated bile acids, taurochenodeoxycholic acid (TCDCA) and Tauro-β-muricholic acid (T-βMCA) (Fig. 4F). Remarkably, compared with DDC group, organic Cr (III) Cr-pic notably reduced T-βMCA level and recovered the level of TCDCA. This underscores that the organic form chromium showcasing superior efficacy than inorganic chromium in altering levels of various bile acids.

3.5. Cr-pic and $CrCl_3$ modulated the gut microbiota to generate BSH for regulating bile acid metabolism and Cr-pic seemed to perturb the abundance of species more than $CrCl_3$

The intestinal microbiota plays a crucial role in the biotransformation of bile acids within the enterohepatic circulation. Fecal 16S rRNA sequencing revealed substantial effects of Cr(III) intervention on the composition and abundance of the gut microbiota. The Shannon, Simpson and Heip index indicated that Cr-pic intervention significantly increased the α-diversity of the gut microbiota in PSC mice compared to control group (Fig. 5A–C). Overall structural changes in the gut microbiota were observed through β-diversity analysis based on PCoA and PLS-DA. PCoA and PLS-DA plots displayed distinct separations between experimental groups, indicating that DDC modeling and Cr(III) intervention altered the composition of the mice gut microbiota (Fig. 5D and E). This emphasizes notable disparities in the intestinal microbial communities among mice subjected to various treatments, with the microbial communities of the different mice groups could be clearly differentiated. Cr(III) intervention was demonstrated to influence the composition of the mice gut microbiota. Composition analysis on genus level revealed the changes in intestinal microbial composition and abundance caused by the intervention of Cr-pic and $CrCl_3$. Among them, the abundances of *Lactobacillus*, *Dubosiella* and *Bifidobacterium* were

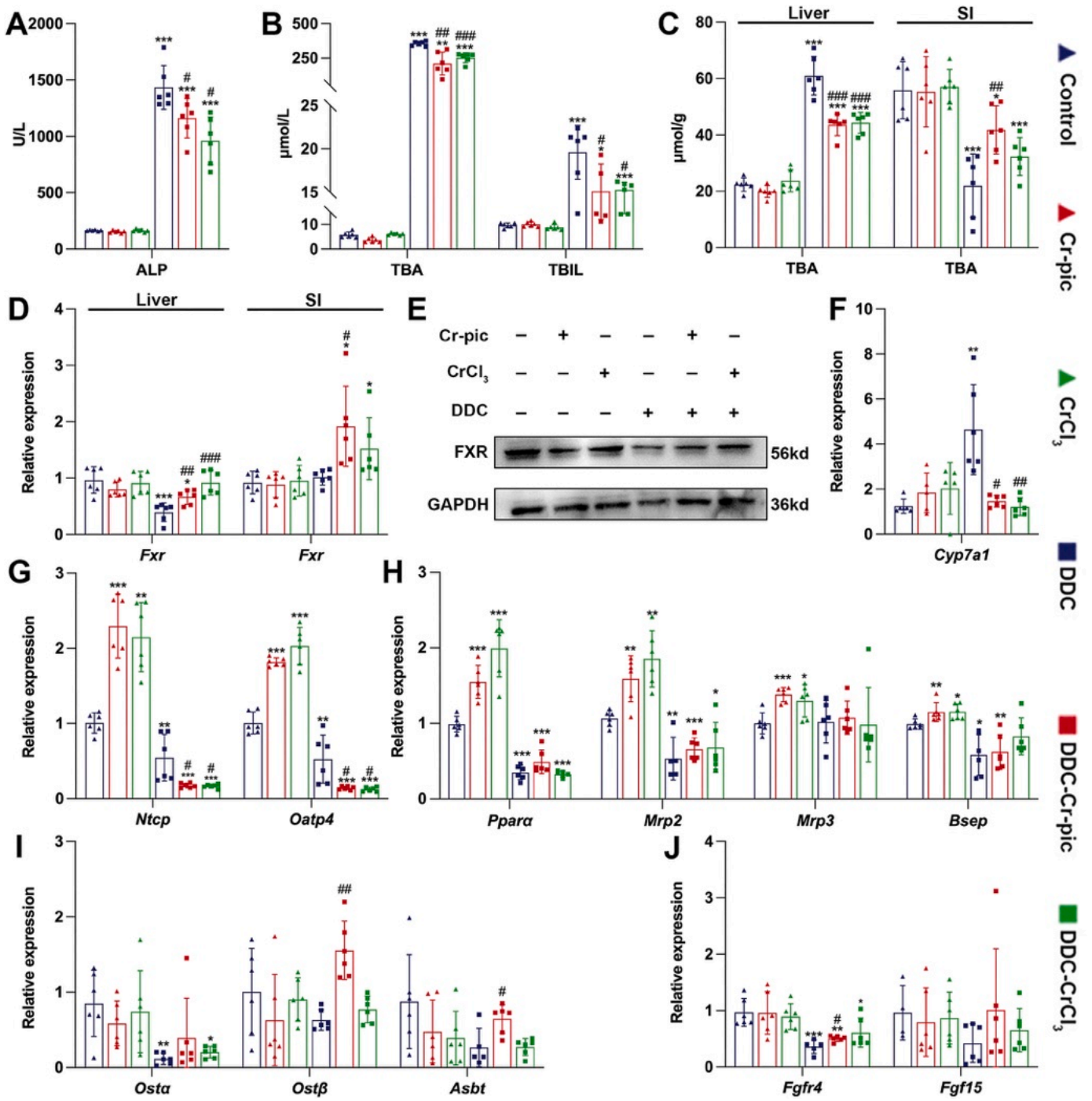

Fig. 3. The impact of Cr-pic and $CrCl_3$ intervention on TBA and bile acid metabolism pathways in PSC mice. (A)The ALP serum level of mice in each group. (B) Concentration of TBIL and TBA in mice serum. (C) TBA levels in liver and small intestine. SI is short for small intestine (D) The expression of *Fxr* in liver and small intestine. (E) Western blot analysis of the FXR expression in liver. (F) The expression of the bile acid synthesis gene *Cyp7a1* in liver. (G) The expression of the bile acid uptake transporter gene *Ntcp* and *Oatp4* in the liver. (H) The expression of the bile acid excretion transporter gene *PPARα*, *Mrp2*, *Mrp3* and *Bsep* in liver. (I) The expression of *Ostα*, *Ostβ* and *Asbt* in small intestine. (J) The expression of *Fgfr4* in liver and the expression of recombinant *Fgf15* in small intestine. (* is the statistical difference compared with the control group, and # is the statistical difference compared with the DDC group; $*p < 0.05$, $**p < 0.01$, $***p < 0.001$; $\#p < 0.05$, $\#\#p < 0.01$, $\#\#\#p < 0.001$).

notably reduced in PSC mice, but increased with Cr(III) intervention. Conversely, the abundances of *Akkermansia*, *unclassified_f_Lachnospiraceae*, *Clostridium_sensu_stricto_1* and *Alistipes* were increased in PSC mice and decreased after Cr(III) intervention (Fig. 5G). Compared with $CrCl_3$, Cr-pic significantly caused perturbations in more genera, including *Dubosiella*, *Bifidobacterium*, and *Turicbacter* in PSC mice. These scenarios illustrate the regulatory effect of Cr(III) intervention on the gut microbial structure in PSC mice. KEGG functional abundance of bile salt hydrolase (BSH) in mouse fecal DNA observed by PICRUSt2 functional prediction, which suggests that in comparison to the control group, the KEGG functional abundance of BSH was notably reduced in the feces of PSC model mice. Nevertheless, after Cr(III) intervention, BSH abundance in mouse feces significantly increased, effectively restoring it to normal levels (Fig. 5H). Correlation

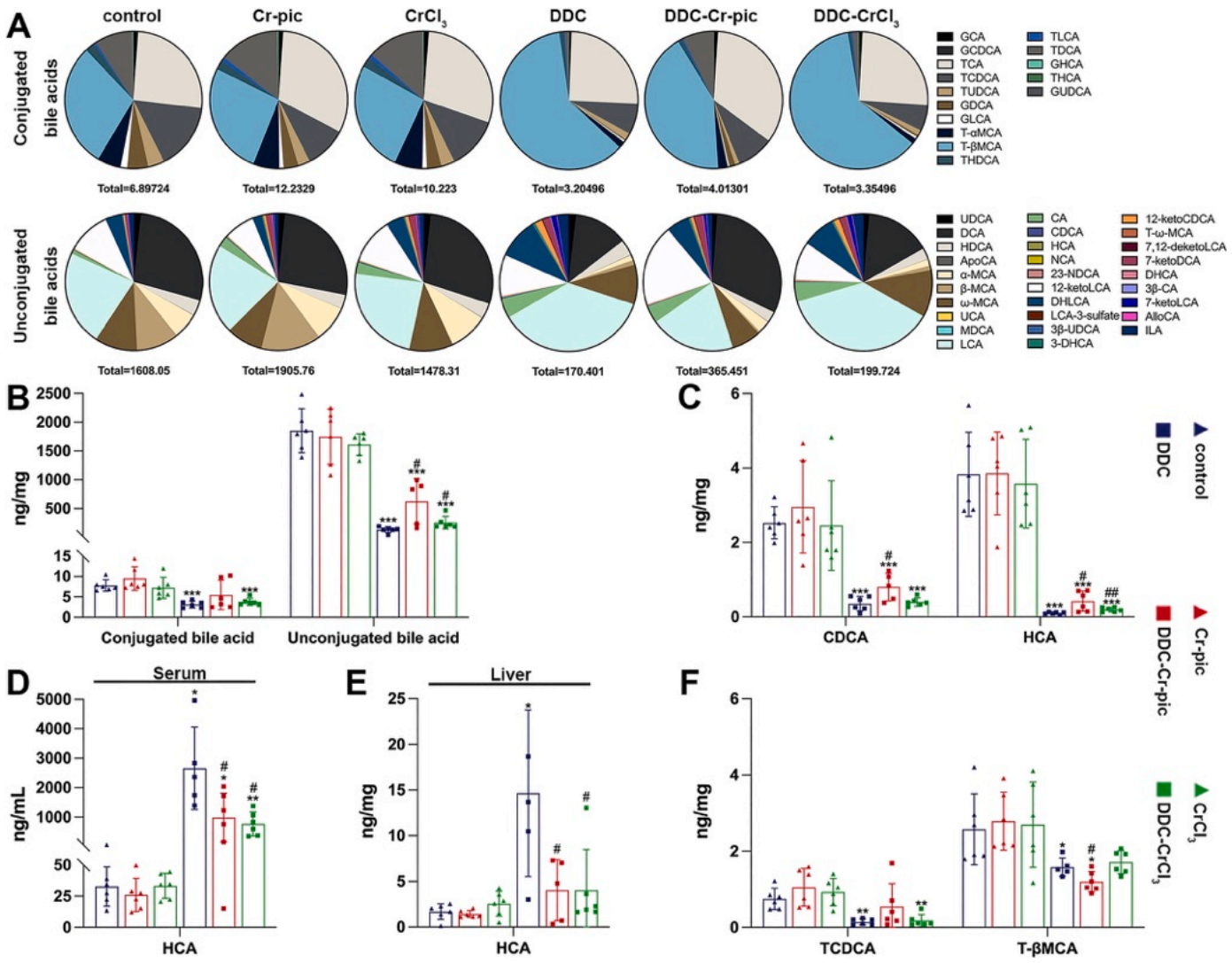

Fig. 4. The content of bile acids of conjugated and unconjugated types was changed after Cr-pic and $CrCl_3$ intervention. (A) Pie chart was used to analyze the abundance ratio and composition of conjugated and unconjugated bile acids after different treatments. (B) Statistics on the total content of conjugated bile acids and unconjugated bile acids. (C) Statistics of changes in concentrations of unconjugated bile acids CDCA and HCA; (D) Statistics of changes in concentrations of HCA in serum; (D) Statistics of changes in concentrations of HCA in liver; (F) Statistics of changes in concentrations of conjugated bile acids TCDCA and T-βMCA. (* is the statistical difference compared with the control group, and # is the statistical difference compared with the DDC group; $*p < 0.05$, $**p < 0.01$, $***p < 0.001$; $\#p < 0.05$, $\#\#p < 0.01$).

analysis revealed a significant positive association between increased genera *Dubosiella*, *Bifidobacterium* and *Turcibacter* in PSC mice supplemented with Cr-pic and the levels of conjugated bile acids CDCA and HCA in feces, suggested that Cr(III) supplementing may through gut microbiota to influence the production and composition of bile acids (Fig. 5I). Above findings indicate that Cr(III) modulates the gut microbiota to generate BSH for regulating bile acid metabolism and Cr-pic which can change the abundance of *Bifidobacterium*, *Dubosiella* and *Turicibacter* in PSC mice seems to align the abundance of species more than $CrCl_3$.

3.6. 6.Cr-pic and $CrCl_3$ improved intestinal damage in PSC mice, Cr-pic functioned better than $CrCl_3$ by improving the intestinal barrier

The length of villus, the depth of crypts and the ratio between them in the ileum was analyzed as a basis for assessing the effect of Cr(III) on the morphology of intestinal mucosa, according to recent study(Liu, Zhao, Zhang, & Nie, 2022). Compared to the control group, there was a significant reduction in ileum villus length in PSC mice, which notably increased after Cr(III) intervention (Fig. 6A–C). The intestinal Histology score basing on the destruction of the epithelial barrier, mucosal damage and inflammatory cell infiltration reveals the disruption of the intestinal tract in DDC-induced PSC mice and the restorative effects of Cr-pic on the intestine (Fig. 6B). Post DDC modeling, the depth of crypts in mouse intestines significantly decreased, and Cr-pic could restore the impact of DDC on crypts (Fig. 6C). The ratio of villus length to crypt depth suggests that Cr-pic and $CrCl_3$ are able to attenuate intestinal mucosal morphology damage (Fig. 6D). The above results indicated that Cr(III) could ameliorate intestinal mucosal morphology damage caused by DDC, with organic Cr(III) Cr-pic demonstrating superior efficacy. To further observe the effect of Cr(III) on the expression of ileal mucosal barrier genes, qPCR analysis was carried out. Results showed that Cr-pic could significantly restore the expression of mucin2 (*Muc2*), occluding (*Ocln*) and claudin-4 (*Cldn4*), which were affected by DDC-induced intestinal barrier damage (Fig. 6E). $CrCl_3$ did not significantly affect the relative expressions of *Muc2*, *Ocln* and *Cldn4* in PSC mice. Results of the above implies that organic Cr(III) Cr-pic is better at restoring intestinal damage in PSC mice compared to inorganic Cr(III). In summary, Cr(III),

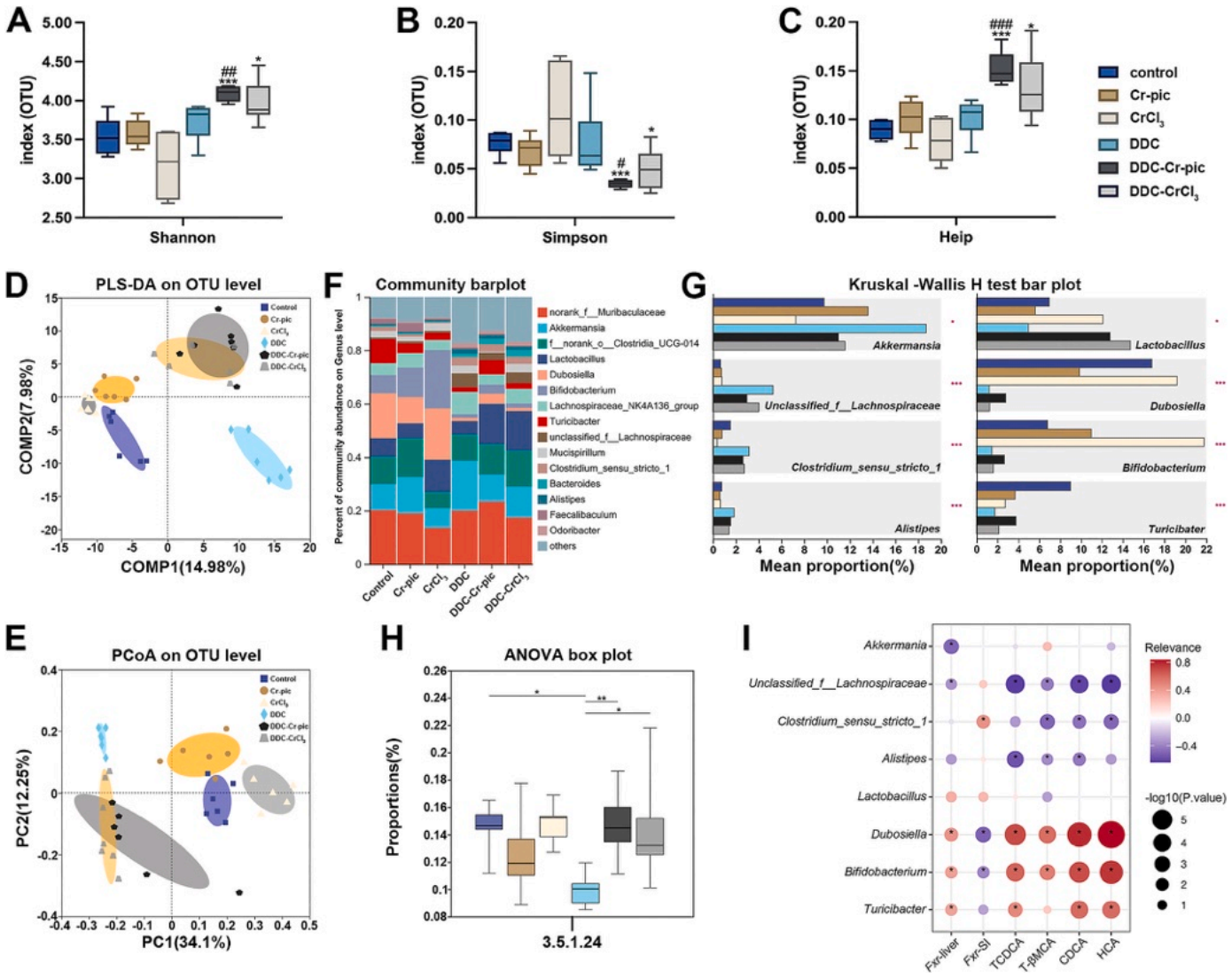

Fig. 5. Analysis of the intestinal microbiome of mice after Cr(III) intervention. (A–C) Alpha diversity index of the intestinal microbiome: Shannon index, Simpson index and Heip index. (D–E) PCoA and PLS-DA analysis of the OTU values of intestinal microbiome in each group. (F) Species composition analysis on genus level. (G) Differential genus in intestinal microbiome sequencing. (H) PICRUSt2 functional prediction for the KEGG functional abundance of the enzyme BSH (3.5.1.24)(Jukes et al., 2020). (I) Partial genera and their correlation analysis heatmap with *Fxr* in the liver and small intestine, as well as bile acids. (* is the statistical difference compared with the control group, and # is the statistical difference compared with the DDC group; $*p < 0.05$, $**p < 0.01$, $***p < 0.001$; $\#p < 0.05$, $\#\#p < 0.01$, $\#\#\#p < 0.001$).

especially Cr-pic, improves the intestinal environment by affecting the villous, crypts and the intestinal barrier, providing conditions for the growth of a wide range of microorganisms and meanwhile provides for the involvement of microorganisms in regulating the bile acid conversion.

4. Discussion

PSC model has characterization of cholestatic liver injury which cause by bile acid metabolism disruption and BAs accumulate in serum and liver. This study revealed that both Cr-pic and $CrCl_3$ intervention as Cr(III) food supplement ameliorated cholestasis of PSC mice in liver and serum, improved the metabolic disorder of BAs. It is worth noting that, as shown in Figs. 3 and 4, Cr-pic alleviated the deficiency of bile acids by activating *Fxr* and reducing T-βMCA in the small intestine of PSC mice. Studies have shown that *Fxr* and *Fgfr4* in liver are responsible for regulating synthesis of bile acid which are secreted into the intestinal and reabsorbed in the ileum, thereby activating intestinal *Fxr*, which leads to the secretion of *Fgf15* in mice (Moreau et al., 2023). In this study, Cr-pic intervention significantly upregulated the expression of *Fgfr4* in the liver of PSC mice, which promoted the regulation of bile acid synthesis and thus activated intestinal *Fxr*, with *Fgf15* also showing increasing trend.Research has indicated that T-βMCA can counter act *Fxr* in the intestine, leading to the DNA damage and proliferation of Lgr5 cells which acts as intestinal stem cells (ISCs) whose proliferation and homeostasis play a crucial role in maintaining the health of the intestinal barrier(Fu et al., 2019; Hu, Yun, Elstrott, & Jasper, 2021; G. Kim et al., 2024; Ma, Chen, Johnston, & Ma, 2022). Thus we speculated the reduction of T-βMCA induce by Cr-pic lead to decreased proliferation of Lgr5 cells and DNA damage repair, and then enhances intestinal barrier function through activing intestinal *Fxr*. CDCA, as one of the *Fxr* agonists, when *Enterobacter aerogenes* ZDY01 reduces the levels of it, has been observed to deactivate *Fxr*(Tang et al., 2022). Meanwhile, administration of CDCA to mice upregulates ileal *Muc2* expression and increases mucosal resident B cell numbers(Tremblay et al., 2017). This suggests that Cr-pic intervention in PSC mice can activate ileal *Fxr* and *Muc2* by elevating CDCA levels, enhancing mucosal resident B cell populations, and restoring the intestinal barrier, consistent with our

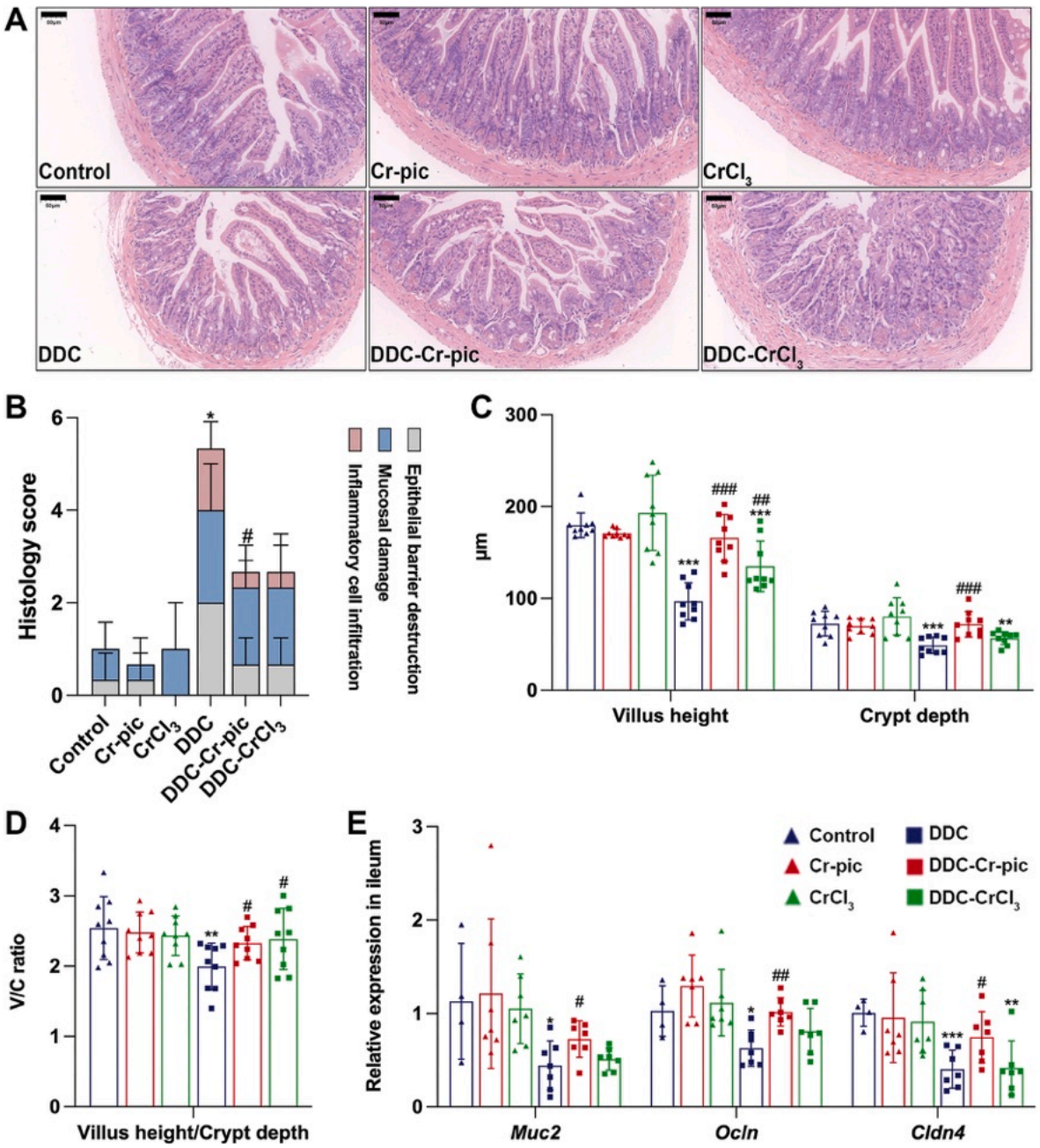

Fig. 6. The impact of Cr(III) intervention on intestinal pathology and barrier in PSC mice. (A) H&E staining of ileum in four groups of mice. (B) Histology score of ileum H&E staining. (C) Villus length and crypt depth of ileum. (D) Villus length to crypt depth ratio of ileum. (E) Expression of intestinal barrier genes *Muc2, Ocln and Cldn4* in ileum. (* is the statistical difference compared with the control group, and # is the statistical difference compared with the DDC group; $^{*}p < 0.05$, $^{**}p < 0.01$, $^{***}p < 0.001$; $\#p < 0.05$, $\#\#p < 0.01$, $\#\#\#p < 0.001$).

experimental results (Figs. 3 and 6). Study pointed out that *Fxr* mitigates inflammation and safeguards the integrity of the intestinal epithelial barrier, this indicates that the restoration of the intestinal barrier in PSC mice by Cr-pic associated with the activation of *Fxr*, whereas $CrCl_3$ failed to activate intestinal *Fxr* could explain why it has a weaker capacity to repair the intestinal barrier(Ding, Yang, Wang, & Huang, 2015). Currently scholars have made different reports for the role between HCA and *Fxr*. One research indicated that HCA can inhibit *Fxr* in enteroendocrine cells to improve glucose homeostasis, the other paper proposed that HCA treatment activated *Fxr* in sheep kidney, researchers used varying intervention concentrations and targets(Z. Zhang et al., 2023; X. Zheng, Cao, et al., 2021). This suggested that HCA may act entirely differently on *Fxr* in diverse tissues or at distinct concentrations. In our experiment, both organic and inorganic forms of Cr(III) increased the content of fecal HCA. Transformation with microbial involvement moderated HCA deficiency in the gut of PSC mice, which may activate intestinal *Fxr*. However, when focusing on changes of HCA in serum and liver, in contrast to the trend of changes in its levels in feces, higher levels may have inhibited hepatic *Fxr*, which was mitigated by the intervention of Cr(III).

Bile acid metabolism is intricately linked to intestinal bacteria, with the gut microbiota playing a critical role in maintaining overall host health(Awoniyi et al., 2023; Collins, Stine, Bisanz, Okafor, & Patterson, 2023; de Vos, Tilg, Van Hul, & Cani, 2022; Fogelson, Dorrestein, Zarrinpar, & Knight, 2023). Patients with PSC exhibit complex alterations in their gut microbiota and its metabolism(Awoniyi et al., 2023; Hole

et al., 2023; Shah, Macdonald, Morrison, & Holtmann, 2020). Germ-free conditions resulted in a 100% mortality rate of *Mdr2* (*Abcb4*) $^{-/-}$ mice by 8 weeks, while selective pathogen-free fecal microbiota transplantation rescued these mice, highlighting the significance of gut microbiota in PSC disease(Awoniyi et al., 2023). The gut microbiota can metabolize primary bile acids produced in the liver through the classical pathway catalyzed by *Cyp7a1* and the alternative pathway catalyzed by cytochrome p450 27a1 (*Cyp27a1*) by deconjugation, resulting in the generation of unconjugated and secondary bile acids and this process promotes the activation of bile acid receptors farnesol x receptor *Fxr* (Rizzolo et al., 2021; Sydor et al., 2020; Torres et al., 2018). Our previous study has certificate that specific gut microbiota could improve PSC symptom by regulating bile acid metabolism through *Fxr*(Shen et al., 2023). Recent studies have found that 6,8-guanidyl luteolin quinone-chromium (GLQ. Cr, an organic form of Cr(III)) can modulate the gut microbiota, thereby helping improve type 2 diabetes(Ge et al., 2023). This suggests that Cr-pic and $CrCl_3$ might modulate the intestinal flora, participate in the influence bile acid metabolism in PSC. This increased microbial diversity after Cr(III) intervention accompanied by the growth of beneficial probiotics, such as *Lactobacillus* and *Bifidobacterium*, as shown in Fig. 5. Cr-pic has a higher growth-promoting capacity for probiotics in the gut than $CrCl_3$, which may result in the formation of more biofilms, enhancing mucosal immunity in the gut, which in turn serves to reinforce the intestinal barrier. Previous studies have shown that reductions in the unconjugated BAs pool and the unconjugated/conjugated BAs ratio are associated with a decreased relative abundance of *Lactobacillus* and *Bifidobacterium* containing the BSH gene(Foley et al., 2021; Gadaleta, Cariello, Crudele, & Moschetta, 2022). Studies have shown that in addition to *Bifidobacterium* and *Lactobacillus*, the bacterial genera of *Enterococcus*, *Clostridium* spp and *Bacteroides* all possess BSH activity(Rimal et al., 2024; Song et al., 2019). Cr(III) supplementation increased the abundance of *Lactobacillus* and *Bacteroides* in PSC mice, with Cr-pic additionally boosting *Bifidobacterium* abundance. This accelerated the deconjugation of bile acids and raised the total unconjugated bile acid levels. Afterwards, bile acids altered by microbial involvement later return to the liver through the portal vein, where they play a role in helping to reduce hepatic inflammation.

Recently, the mechanisms of PSC are being explored and several mainstream theories about the pathogenesis of this disease have been put forward(Y. S. Kim et al., 2023; Little et al., 2020). The initiation of liver autoimmunity may be the key to PSC(Assis et al., 2023; Park et al., 2022). In PSC patients, pathogens invade the intestinal mucosa into the portal vein and induce the occurrence of liver autoimmune response(Cai et al., 2022). Macrophages, neutrophils dendritic cells and NK cells are activated by invaded pathogen, and they secret cytokines *Tnfα*, *Il-1β* and chemokine *Cxcl8* to recruit lymphocytes to maintain inflammation(van Munster, Bergquist, & Ponsioen, 2023). Among them, bile duct epithelial cells (BECS) play an important role in pro-inflammatory and pro-fibrotic responses by overexpression of reactive phenotypes of adhesion molecules to production and secretion of pro-inflammatory and chemotactic cytokines and growth factors, further accelerating the inflammatory process(Trivedi & Hirschfield, 2021). Prior research has identified a significant accumulation of macrophages in liver samples from patients with PSC compared to health people(Guicciardi et al., 2018). Studies have indicated that BECs expressed *Cx3cl1* and *Ccl2* to recruit macrophages to the bile ducts in PSC patients, then these macrophages increased the expression of *iNOS* show proinflammatory phenotype(Trussoni & LaRusso, 2023). Previous studies have identified increased peribiliary proinflammatory (M1-like) macrophages (one of activated macrophages, secrete various pro-inflammatory cytokines such as *Tnfα* to promote liver inflammation and liver injury) in PSC compared to normal livers(Gharavi, Hanjani, Movahed, & Doroudian, 2022; Guicciardi et al., 2018; Wang et al., 2021; J. Zhang et al., 2022). Similarly, as shown in Fig. 2, our study found that both $CrCl_3$ and Cr-pic treatment showed marked histopathological improvement on anti-inflammation in liver accompany with a notable reduction in the number of macrophages in the livers of PSC mice. Nevertheless, further analysis of pro-inflammatory macrophages yielded an intriguing finding: Cr-pic was capable of decreasing the number of M1-polarized macrophages and the expression of cytokines *Tnfα*, *iNOS* and *Cxcl10*. A finding consistent with our own study verified that Cr-pic could decrease pro-inflammatory cytokines *Il-6* and *Tnfα* in rheumatoid arthritis (RA) patients. Recent studies have shown macrophages can be reduced by bile acid to reduce LPS-induced secretion of pro-inflammatory cytokines such as *Tnfα*, participate in macrophage polarization, among them, TCDCA has been reported to inhibit inflammation(Bao et al., 2021; Qi et al., 2020; Shao et al., 2022). This suggests that Cr-pic perturbed the levels of various bile acids such as TCDCA more than $CrCl_3$, possibly reducing M1-type polarization through changes in bile acids.

CRediT authorship contribution statement

Yu Shen: Writing – original draft, Visualization, Software, Formal analysis, Data curation. **Baorong Jiang:** Validation, Software, Formal analysis, Data curation. **Zejia Hao:** Validation, Software, Formal analysis, Data curation. **Chenchen Zhang:** Validation, Software, Formal analysis, Data curation. **Zhan Zhang:** Validation, Software, Formal analysis. **Qian Wu:** Validation, Software, Methodology, Formal analysis. **Lei Li:** Writing – review & editing, Visualization, Supervision, Resources, Project administration, Funding acquisition, Conceptualization. **Ping Jiang:** Writing – review & editing, Visualization, Supervision, Project administration, Methodology, Funding acquisition, Conceptualization.

Declaration of competing interest

The authors declare that they have no known competing financial interests or personal relationships that could have appeared to influence the work reported in this paper.

Data availability

Data will be made available on request.

Acknowledgment

This work was supported by the National Natural Science Foundation of China (No. 82173571).

Appendix A. Supplementary data

Supplementary data to this article can be found online at https://doi.org/10.1016/j.fbio.2024.104887.

References

Ali, A. H., Carey, E. J., & Lindor, K. D. (2016). The microbiome and primary sclerosing cholangitis. *Seminars in Liver Disease, 36*(4), 340–348. https://doi.org/10.1055/s-0036-1594007

Assis, D. N., & Bowlus, C. L. (2023). Recent advances in the management of primary sclerosing cholangitis. *Clinical Gastroenterology and Hepatology, 21*(8), 2065–2075. https://doi.org/10.1016/j.cgh.2023.04.004

Awoniyi, M., Wang, J., Ngo, B., Meadows, V., Tam, J., Viswanathan, A., … Sartor, R. B. (2023). Protective and aggressive bacterial subsets and metabolites modify hepatobiliary inflammation and fibrosis in a murine model of PSC. *Gut, 72*(4), 671–685. https://doi.org/10.1136/gutjnl-2021-326500

Bao, L., Hao, D., Wang, X., He, X., Mao, W., & Li, P. (2021). Transcriptome investigation of anti-inflammation and immuno-regulation mechanism of taurochenodeoxycholic acid. *BMC Pharmacol Toxicol, 22*(1), 23. https://doi.org/10.1186/s40360-021-00491-0

Cai, J., Rimal, B., Jiang, C., Chiang, J. Y. L., & Patterson, A. D. (2022). Bile acid metabolism and signaling, the microbiota, and metabolic disease. *Pharmacol Ther, 237*, Article 108238. https://doi.org/10.1016/j.pharmthera.2022.108238

Collins, S. L., Stine, J. G., Bisanz, J. E., Okafor, C. D., & Patterson, A. D. (2023). Bile acids and the gut microbiota: Metabolic interactions and impacts on disease. *Nature Reviews Microbiology, 21*(4), 236–247. https://doi.org/10.1038/s41579-022-00805-x

de Vos, W. M., Tilg, H., Van Hul, M., & Cani, P. D. (2022). Gut microbiome and health: Mechanistic insights. *Gut, 71*(5), 1020–1032. https://doi.org/10.1136/gutjnl-2021-326789

Deng, X., Zhang, X., Li, W., Feng, R. X., Li, L., Yi, G. R., … Xie, W. F. (2018). Chronic liver injury induces conversion of biliary epithelial cells into hepatocytes. *Cell Stem Cell, 23*(1), 114–122.e113. https://doi.org/10.1016/j.stem.2018.05.022

Di Vincenzo, F., Del Gaudio, A., Petito, V., Lopetuso, L. R., & Scaldaferri, F. (2023). Gut microbiota, intestinal permeability, and systemic inflammation: A narrative review. *Intern Emerg Med*. https://doi.org/10.1007/s11739-023-03374-w

Ding, L., Yang, L., Wang, Z., & Huang, W. (2015). Bile acid nuclear receptor FXR and digestive system diseases. *Acta Pharmaceutica Sinica B, 5*(2), 135–144. https://doi.org/10.1016/j.apsb.2015.01.004

Feng, W., Li, Q., Wang, W., Chen, Y., Zhang, W., Zhao, T., … Yang, L. (2019). Influence of chronic toxicity, lipid metabolism, learning and memory ability, and related enzyme in sprague-dawley rats by long-term chromium malate supplementation. *Biological Trace Element Research, 187*(1), 243–257. https://doi.org/10.1007/s12011-018-1377-z

Fickert, P., Stöger, U., Fuchsbichler, A., Moustafa, T., Marschall, H. U., Weiglein, A. H., … Trauner, M. (2007). A new xenobiotic-induced mouse model of sclerosing cholangitis and biliary fibrosis. *Am J Pathol, 171*(2), 525–536. https://doi.org/10.2353/ajpath.2007.061133

Fogelson, K. A., Dorrestein, P. C., Zarrinpar, A., & Knight, R. (2023). The gut microbial bile acid modulation and its relevance to digestive health and diseases. *Gastroenterology, 164*(7), 1069–1085. https://doi.org/10.1053/j.gastro.2023.02.022

Foley, M. H., O'Flaherty, S., Allen, G., Rivera, A. J., Stewart, A. K., Barrangou, R., et al. (2021). Lactobacillus bile salt hydrolase substrate specificity governs bacterial fitness and host colonization. *Proc Natl Acad Sci U S A, 118*(6). https://doi.org/10.1073/pnas.2017709118

Fu, T., Coulter, S., Yoshihara, E., Oh, T. G., Fang, S., Cayabyab, F., … Evans, R. M. (2019). FXR regulates intestinal cancer stem cell proliferation. *Cell, 176*(5), 1098–1112.e1018. https://doi.org/10.1016/j.cell.2019.01.036

Gadaleta, R. M., Cariello, M., Crudele, L., & Moschetta, A. (2022). Bile salt hydrolase-competent probiotics in the management of IBD: Unlocking the "bile acid code. *Nutrients, 14*(15). https://doi.org/10.3390/nu14153212

Ge, X., He, X., Liu, J., Zeng, F., Chen, L., Xu, W., … Liu, B. (2023). Amelioration of type 2 diabetes by the novel 6, 8-guanidyl luteolin quinone-chromium coordination via biochemical mechanisms and gut microbiota interaction. *Journal of Advanced Research, 46*, 173–188. https://doi.org/10.1016/j.jare.2022.06.003

Gharavi, A. T., Hanjani, N. A., Movahed, E., & Doroudian, M. (2022). The role of macrophage subtypes and exosomes in immunomodulation. *Cell Mol Biol Lett, 27*(1), 83. https://doi.org/10.1186/s11658-022-00384-y

Guicciardi, M. E., Trussoni, C. E., Krishnan, A., Bronk, S. F., Lorenzo Pisarello, M. J., O'Hara, S. P., … Gores, G. J. (2018). Macrophages contribute to the pathogenesis of sclerosing cholangitis in mice. *Journal of Hepatology, 69*(3), 676–686. https://doi.org/10.1016/j.jhep.2018.05.018

Hole, M. J., Jørgensen, K. K., Holm, K., Braadland, P. R., Meyer-Myklestad, M. H., Medhus, A. W., … Hov, J. R. (2023). A shared mucosal gut microbiota signature in primary sclerosing cholangitis before and after liver transplantation. *Hepatology, 77*(3), 715–728. https://doi.org/10.1002/hep.32773

Hov, J. R., & Karlsen, T. H. (2023). The microbiota and the gut-liver axis in primary sclerosing cholangitis. *Nature Reviews Gastroenterology & Hepatology, 20*(3), 135–154. https://doi.org/10.1038/s41575-022-00690-y

Hu, D. J., Yun, J., Elstrott, J., & Jasper, H. (2021). Non-canonical Wnt signaling promotes directed migration of intestinal stem cells to sites of injury. *Nature Communications, 12*(1), 7150. https://doi.org/10.1038/s41467-021-27384-4

Jukes, C. A., Ijaz, U. Z., Buckley, A., Spencer, J., Irvine, J., Candlish, D., … Douce, G. (2020). Bile salt metabolism is not the only factor contributing to Clostridioides (Clostridium) difficile disease severity in the murine model of disease. *Gut Microbes, 11*(3), 481–496. https://doi.org/10.1080/19490976.2019.1678996

Katanasaka, Y., Yabe, H., Murata, N., Sobukawa, M., Sugiyama, Y., Sato, H., … Morimoto, T. (2024). Fibroblast-specific PRMT5 deficiency suppresses cardiac fibrosis and left ventricular dysfunction in male mice. *Nature Communications, 15*(1), 2472. https://doi.org/10.1038/s41467-024-46711-z

Kim, G., Chen, Z., Li, J., Luo, J., Castro-Martinez, F., Wisniewski, J., … Wu, C. (2024). Gut-liver axis calibrates intestinal stem cell fitness. *Cell, 187*(4), 914–930.e920. https://doi.org/10.1016/j.cell.2024.01.001

Kim, Y. S., Hurley, E. H., Park, Y., & Ko, S. (2023). Primary sclerosing cholangitis (PSC) and inflammatory bowel disease (IBD): A condition exemplifying the crosstalk of the gut-liver axis. *Exp Mol Med, 55*(7), 1380–1387. https://doi.org/10.1038/s12276-023-01042-9

Li, Y., Wei, L., Zhang, P., Xiao, J., Guo, Z., & Fu, Q. (2022). Bioaccumulation of dietary CrPic, Cr(III) and Cr(VI) in juvenile coral trout (Plectropomus leopardus). *Ecotoxicology and Environmental Safety, 240*, Article 113692. https://doi.org/10.1016/j.ecoenv.2022.113692

Lin, S., Wang, S., Wang, P., Tang, C., Wang, Z., Chen, L., … Fang, Z. (2023). Bile acids and their receptors in regulation of gut health and diseases. *Progress in Lipid Research, 89*, Article 101210. https://doi.org/10.1016/j.plipres.2022.101210

Little, R., Wine, E., Kamath, B. M., Griffiths, A. M., & Ricciuto, A. (2020). Gut microbiome in primary sclerosing cholangitis: A review. *World Journal of Gastroenterology, 26*(21), 2768–2780. https://doi.org/10.3748/wjg.v26.i21.2768

Liu, H., Zhao, J., Zhang, W., & Nie, C. (2022). Impacts of sodium butyrate on intestinal mucosal barrier and intestinal microbial community in a weaned piglet model. *Frontiers in Microbiology, 13*, Article 1041885. https://doi.org/10.3389/fmicb.2022.1041885

Ma, N., Chen, X., Johnston, L. J., & Ma, X. (2022). Gut microbiota-stem cell niche crosstalk: A new territory for maintaining intestinal homeostasis. *Imeta, 1*(4), e54. https://doi.org/10.1002/imt2.54

Ma, N., Guo, P., Chen, J., Qi, Z., Liu, C., Shen, J., … Ma, X. (2023). Poly-β-hydroxybutyrate alleviated diarrhea and colitis via Lactobacillus johnsonii biofilm-mediated maturation of sulfomucin. *Science China Life Sciences, 66*(7), 1569–1588. https://doi.org/10.1007/s11427-022-2213-6

Mooney, K. W., & Cromwell, G. L. (1997). Efficacy of chromium picolinate and chromium chloride as potential carcass modifiers in swine. *Journal of Animal Science, 75*(10), 2661–2671. https://doi.org/10.2527/1997.75102661x

Moreau, F., Brunao, B. B., Liu, X. Y., Tremblay, F., Fitzgerald, K., Avila-Pacheco, J., … Softic, S. (2023). Liver-specific FGFR4 knockdown in mice on an HFD increases bile acid synthesis and improves hepatic steatosis. *The Journal of Lipid Research, 64*(2), Article 100324. https://doi.org/10.1016/j.jlr.2022.100324

Nishimura, K., Iitaka, S., & Nakagawa, H. (2021). Effect of trivalent chromium on erythropoietin production and the prevention of insulin resistance in HepG2 cells. *Archives of Biochemistry and Biophysics, 708*, Article 108960. https://doi.org/10.1016/j.abb.2021.108960

Nussbaumerova, B., Rosolova, H., Krizek, M., Sefrna, F., Racek, J., Müller, L., et al. (2018). Chromium supplementation reduces resting heart rate in patients with metabolic syndrome and impaired glucose tolerance. *Biological Trace Element Research, 183*(2), 192–199. https://doi.org/10.1007/s12011-017-1128-6

Park, J. W., Kim, J. H., Kim, S. E., Jung, J. H., Jang, M. K., Park, S. H., … Kim, D. J. (2022). Primary biliary cholangitis and primary sclerosing cholangitis: Current knowledge of pathogenesis and therapeutics. *Biomedicines, 10*(6). https://doi.org/10.3390/biomedicines10061288

Qi, Y. C., Duan, G. Z., Mao, W., Liu, Q., Zhang, Y. L., & Li, P. F. (2020). Taurochenodeoxycholic acid mediates cAMP-PKA-CREB signaling pathway. *Chinese Journal of Natural Medicines, 18*(12), 898–906. https://doi.org/10.1016/s1875-5364(20)60033-4

Rimal, B., Collins, S. L., Tanes, C. E., Rocha, E. R., Granda, M. A., Solanki, S., … Patterson, A. D. (2024). Bile salt hydrolase catalyses formation of amine-conjugated bile acids. *Nature, 626*(8000), 859–863. https://doi.org/10.1038/s41586-023-06990-w

Rizzolo, D., Kong, B., Taylor, R. E., Brinker, A., Goedken, M., Buckley, B., et al. (2021). Bile acid homeostasis in female mice deficient in Cyp7a1 and Cyp27a1. *Acta Pharmaceutica Sinica B, 11*(12), 3847–3856. https://doi.org/10.1016/j.apsb.2021.05.023

Shah, A., Macdonald, G. A., Morrison, M., & Holtmann, G. (2020). Targeting the gut microbiome as a treatment for primary sclerosing cholangitis: A conceptional framework. *American Journal of Gastroenterology, 115*(6), 814–822. https://doi.org/10.14309/ajg.0000000000000604

Shao, J., Ge, T., Tang, C., Wang, G., Pang, L., & Chen, Z. (2022). Synergistic anti-inflammatory effect of gut microbiota and lithocholic acid on liver fibrosis. *Inflammation Research, 71*(10–11), 1389–1401. https://doi.org/10.1007/s00011-022-01629-4

Shen, Y., Jiang, B., Zhang, C., Wu, Q., Li, L., & Jiang, P. (2023). Combined inhibition of the TGF-β1/smad pathway by prevotella copri and Lactobacillus murinus to reduce inflammation and fibrosis in primary sclerosing cholangitis. *International Journal of Molecular Sciences, 24*(13). https://doi.org/10.3390/ijms241311010

Song, Z., Cai, Y., Lao, X., Wang, X., Lin, X., Cui, Y., … Li, J. (2019). Taxonomic profiling and populational patterns of bacterial bile salt hydrolase (BSH) genes based on worldwide human gut microbiome. *Microbiome, 7*(1), 9. https://doi.org/10.1186/s40168-019-0628-3

Sun, J., Fan, J., Li, T., Yan, X., & Jiang, Y. (2022). Nuciferine protects against high-fat diet-induced hepatic steatosis via modulation of gut microbiota and bile acid metabolism in rats. *Journal of Agricultural and Food Chemistry, 70*(38), 12014–12028. https://doi.org/10.1021/acs.jafc.2c04817

Sydor, S., Manka, P., van Buren, L., Theurer, S., Schwertheim, S., Best, J., … Bechmann, L. P. (2020). Hepatocyte KLF6 expression affects FXR signalling and the clinical course of primary sclerosing cholangitis. *Liver International, 40*(9), 2172–2181. https://doi.org/10.1111/liv.14542

Tang, J., Qin, M., Tang, L., Shan, D., Zhang, C., Zhang, Y., … Yu, J. (2022). Correction: Enterobacter aerogenes ZDY01 inhibits choline-induced atherosclerosis through CDCA-FXR-FGF15 axis. *Food Funct, 13*(1), 459. https://doi.org/10.1039/d1fo90118d

Torres, J., Palmela, C., Brito, H., Bao, X., Ruiqi, H., Moura-Santos, P., … Hu, J. (2018). The gut microbiota, bile acids and their correlation in primary sclerosing cholangitis associated with inflammatory bowel disease. *United European Gastroenterol J, 6*(1), 112–122. https://doi.org/10.1177/2050640617708953

Tremblay, S., Romain, G., Roux, M., Chen, X. L., Brown, K., Gibson, D. L., … Menendez, A. (2017). Bile acid administration elicits an intestinal antimicrobial program and reduces the bacterial burden in two mouse models of enteric infection. *Infection and Immunity, 85*(6). https://doi.org/10.1128/iai.00942-16

Trivedi, P. J., & Hirschfield, G. M. (2021). Recent advances in clinical practice: Epidemiology of autoimmune liver diseases. *Gut, 70*(10), 1989–2003. https://doi.org/10.1136/gutjnl-2020-322362

Trussoni, C. E., & LaRusso, N. F. (2023). Macrophages make a difference in cholestatic liver diseases - but how? *Journal of Hepatology*. https://doi.org/10.1016/j.jhep.2023.09.022

Tveter, K. M., Mezhibovsky, E., Wu, Y., & Roopchand, D. E. (2023). Bile acid metabolism and signaling: Emerging pharmacological targets of dietary polyphenols. *Pharmacol Ther, 248*, Article 108457. https://doi.org/10.1016/j.pharmthera.2023.108457

van Munster, K. N., Bergquist, A., & Ponsioen, C. Y. (2023). Inflammatory bowel disease and primary sclerosing cholangitis: One disease or two? *Journal of Hepatology*. https://doi.org/10.1016/j.jhep.2023.09.031

Vincent, J. B., & Lukaski, H. C. (2018). Chromium. *Advances in Nutrition, 9*(4), 505–506. https://doi.org/10.1093/advances/nmx021

Wang, C., Ma, C., Gong, L., Guo, Y., Fu, K., Zhang, Y., … Li, Y. (2021). Macrophage polarization and its role in liver disease. *Frontiers in Immunology, 12*, Article 803037. https://doi.org/10.3389/fimmu.2021.803037

White, P. E., & Vincent, J. B. (2019). Systematic review of the effects of chromium(III) on chickens. *Biological Trace Element Research, 188*(1), 99–126. https://doi.org/10.1007/s12011-018-1575-8

Willoughby, D., Hewlings, S., & Kalman, D. (2018). Body composition changes in weight loss: Strategies and supplementation for maintaining lean body mass, a brief review. *Nutrients, 10*(12). https://doi.org/10.3390/nu10121876

Zhang, J., Liu, Y., Chen, H., Yuan, Q., Wang, J., Niu, M., … Zhang, J. (2022). MyD88 in hepatic stellate cells enhances liver fibrosis via promoting macrophage M1 polarization. *Cell Death & Disease, 13*(4), 411. https://doi.org/10.1038/s41419-022-04802-z

Zhang, Z., Zhang, B., Jiang, X., Yu, Y., Cui, Y., Luo, H., et al. (2023). Hyocholic acid retards renal fibrosis by regulating lipid metabolism and inflammatory response in a sheep model. *International Immunopharmacology, 122*, Article 110670. https://doi.org/10.1016/j.intimp.2023.110670

Zhao, Y., He, X., Ma, X., Wen, J., Li, P., Wang, J., … Xiao, X. (2017). Paeoniflorin ameliorates cholestasis via regulating hepatic transporters and suppressing inflammation in ANIT-fed rats. *Biomedicine & Pharmacotherapy, 89*, 61–68. https://doi.org/10.1016/j.biopha.2017.02.025

Zheng, S., Cao, P., Yin, Z., Wang, X., Chen, Y., Yu, M., … Yang, X. (2021a). Apigenin protects mice against 3,5-diethoxycarbonyl-1,4-dihydrocollidine-induced cholestasis. *Food Funct, 12*(5), 2323–2334. https://doi.org/10.1039/d0fo02910f

Zheng, X., Chen, T., Jiang, R., Zhao, A., Wu, Q., Kuang, J., … Jia, W. (2021b). Hyocholic acid species improve glucose homeostasis through a distinct TGR5 and FXR signaling mechanism. *Cell Metabolism, 33*(4), 791–803.e797. https://doi.org/10.1016/j.cmet.2020.11.017

Zheng, H., Hu, Y., Shao, M., Chen, S., & Qi, S. (2023). Chromium picolinate protects against testicular damage in STZ-induced diabetic rats via anti-inflammation, anti-oxidation, inhibiting apoptosis, and regulating the TGF-$\hat{I}^2$1/smad pathway. *Molecules, 28*(22). https://doi.org/10.3390/molecules28227669